Emergent Prethermalization Signatures in Out-of-Time Ordered Correlations

Ken Xuan Wei,[1] Pai Peng (彭湃),[2] Oles Shtanko,[1] Iman Marvian,[3] Seth Lloyd,[4]
Chandrasekhar Ramanathan,[5] and Paola Cappellaro[6,*]

[1]*Department of Physics, Massachusetts Institute of Technology, Cambridge, Massachusetts 02139, USA*
[2]*Department of Electrical Engineering and Computer Science, Massachusetts Institute of Technology, Cambridge, Massachusetts 02139, USA*
[3]*Departments of Physics & Electrical and Computer Engineering, Duke University, Durham, North Carolina 27708, USA*
[4]*Department of Mechanical Engineering, Massachusetts Institute of Technology, Cambridge, Massachusetts 02139, USA*
[5]*Department of Physics and Astronomy, Dartmouth College, Hanover, New Hampshire 03755, USA*
[6]*Department of Nuclear Science and Engineering, Massachusetts Institute of Technology, Cambridge, Massachusetts 02139, USA*

(Received 11 December 2018; published 30 August 2019)

How a many-body quantum system thermalizes—or fails to do so—under its own interaction is a fundamental yet elusive concept. Here we demonstrate nuclear magnetic resonance observation of the emergence of prethermalization by measuring out-of-time ordered correlations. We exploit Hamiltonian engineering techniques to tune the strength of spin-spin interactions and of a transverse magnetic field in a spin chain system, as well as to invert the Hamiltonian sign to reveal out-of-time ordered correlations. At large fields, we observe an emergent conserved quantity due to prethermalization, which can be revealed by an early saturation of correlations. Our experiment not only demonstrates a new protocol to measure out-of-time ordered correlations, but also provides new insights in the study of quantum thermodynamics.

DOI: 10.1103/PhysRevLett.123.090605

The dynamics of many-body quantum systems can display a multitude of interesting phenomena, ranging from thermalization [1,2] to many-body localization (MBL) [3–10], discrete time crystals [11–19], and dynamical phase transitions [20–25]. Recently, there has been increased interest in systems exhibiting nonergodic dynamics in the absence of any disorder or incommensurate fields, such as quasi-MBL in translationally invariant systems [26] and disorder free localization [27–29]. Another intriguing possibility is prethermalization, where nonintegrable quantum systems may fail to thermalize on practically accessible timescales [30–35], due to an emergent quasilocal integral of motion.

Here we study thermalization and prethermalization by measuring out-of-time-ordered (OTO) commutators, which have been used to study many quantum thermalization phenomena, such as scrambling [36–41], many-body localization [42–45], and integrability [40]. OTO commutators are powerful indicators of information scrambling, but are typically difficult to observe experimentally.

We exploit Hamiltonian engineering techniques to investigate the onset of prethermalization in a nuclear spin system in a natural crystal. We can access different regimes by manipulating the relative strengths of the dipolar interactions among spins and the transverse magnetic field. After a quench, we experimentally measure OTO commutators using multiple quantum coherence (MQC) experiments [9,46,47] for a system initially at an effective infinite temperature. In the low field regime, the commutator keeps increasing, indicating the system thermalizes in the observed timescale. In the high field regime, a long-lived prethermal regime arises due to an emergent conserved quantity and the OTO commutator involving such a prethermal conserved quantity saturates after a short time. We further support the interpretation of our experimental results by constructing the prethermal Hamiltonian perturbatively [34,48]. We numerically observe the divergence of the perturbation series below a certain transverse field threshold, indicating the breakdown of prethermal dynamics and the onset of the thermal regime.

We work with nuclear spins in fluorapatite (FAp) [49], an experimental system recently used to show MBL [9]. The ^{19}F spins-1/2 form linear chains in the crystal and are coupled by the magnetic dipolar interaction. A single crystal is placed in a large (7 T) magnetic field at room temperature. In a strong magnetic field the interaction Hamiltonian for the ^{19}F spins is given by the secular dipolar Hamiltonian $H_{\mathrm{dip}z} = \sum_{j,k>j} J_{jk}[S_z^j S_z^k - \frac{1}{2}(S_x^j S_x^k + S_y^j S_y^k)]$, where $J_{jk} = J|j-k|^{-3}$. Here $S_\alpha^j (\alpha = x, y, z)$ are spin-1/2 operators of the jth ^{19}F spin (see Section I in the Supplemental Material [50]). In the timescales we explore, the system can be approximately treated as an ensemble of identical spin chains [51–53], since the interchain coupling is ∼40 times weaker than the intrachain coupling. The signal is averaged over a macroscopic number of chains in

the crystal, with an average chain length L larger than 50, much longer than the extent of correlation in the experiments. The coupling to ^{31}P spins in the lattice is refocused by the applied control, and the spin-lattice relaxation effects are negligible ($T_1 \approx 0.8$ s). The dynamics of the ^{19}F spins are thus well approximated by a 1D closed quantum system with dipolar couplings. While the corresponding 1D, nearest-neighbor XXZ Hamiltonian is integrable [54–56], the Hamiltonian we consider can lead to diffusive [57,58] and chaotic behavior [59] in 3D. In the presence of a transverse field, the system is known to show a quantum phase transition [60].

In experiments we consider the dynamics under an engineered Floquet Hamiltonian, obtained by modulating $H_{\mathrm{dip}z}$ with periodic sequences of strong rf pulse [61] that can also introduce quenches and time reversal. To lowest order of Magnus expansion the pulse sequence (see Section II in the Supplemental Material [50]) engineers a dipolar Hamiltonian along the y direction, $H_{\mathrm{dip}y}$ [9], while an effective static transverse field is introduced by phase shifting all the pulses. The resulting Floquet-Trotter Hamiltonian is equivalent to its lowest order to a transverse field dipolar Hamiltonian $H_{\mathrm{tdip}} = uH_{\mathrm{dip}y} + gZ$ [62]:

$$H_{\mathrm{tdip}} = u\sum_{j,k>j} J_{jk}\left[S_y^j S_y^k - \frac{1}{2}(S_x^j S_x^k + S_z^j S_z^k)\right] + g\sum_j S_z^j \quad (1)$$

where both u and g are under experimental control (for details see Section II in the Supplemental Material [50]) and we set $J = -uJ_{j,j+1}$ being the engineered nearest-neighbor coupling strength. In all experiments we set $u = 0.2$ and pulse sequence period $t_c = 96$ μs, which corresponds to an effective $Jt_c = 0.62$, given the natural $J_{j,j+1} = -33$ krad/s neighbor coupling strength in fluorapatite. For either $g = 0$ or $J = 0$ the magnetizations $Y = \sum_j S_y^j$ and $Z = \sum_j S_z^j$ are exactly conserved, respectively. Although prethermalization is expected when moving away both limits, their dynamics differ both fundamentally and practically. At low field $g/J \ll 1$, the heating rate from prethermal state to thermal state is quadratic $\propto (g/J)^2$, which can be explained by the time-independent perturbation theory [64], while the prethermalization at large field $g/J \gg 1$ features exponentially small heating rate $\propto \exp(-O(g/J))$, which is of the same origin as Floquet prethermalization [34,65]. The difference is observed in the experimental two point correlators $\langle Z(t)Z\rangle_{\beta=0}$ and $\langle Y(t)Y\rangle_{\beta=0}$ shown in Fig. 1(a). In this Letter, we focus on the exponentially slow heating at a large field regime. As shown in Ref. [66], a prethermal regime exists for Hamiltonians that can be divided into two parts $H = H_0 + \epsilon V$, with H_0 having integer eigenvalues up to a scaling factor C, $e^{i2\pi CH_0} = \mathbb{1}$. For sufficiently small ϵ, H can be approximately transformed to a prethermal Hamiltonian H_{pre}, through a local unitary R [34,65], i.e., $RHR^\dagger = H_{\mathrm{pre}} + \delta H$, where δH is exponentially small in ϵ, $R = \mathbb{1} + O(\epsilon)$, and $[H_0', H_{\mathrm{pre}}] = 0$, where H_0' in the frame rotated by R has the same matrix representation as H_0 in the original frame, so they are different physical operators. As the prethermal Hamiltonian conserves H_0', $R^\dagger H_0' R$ is a conserved quantity in the original frame up to an exponentially long time t_{pre}, after which the small correction δH thermalizes the system. In the transverse field dipolar model with $g \gg J$, we can identify the dominant part with the field and the perturbation with the dipolar interaction. The prethermal Hamiltonian is then $H_{\mathrm{pre}} = gZ' - uH_{\mathrm{dip}z}'/2 + O(J^2/g)$. Then, in the prethermal regime we expect an emergent conserved quantity, Z_{pre}, related to Z' by a local unitary transformation R, $Z_{\mathrm{pre}} = R^\dagger Z' R$.

To investigate the presence of this emergent constant of motion beyond the partial information given by local observables [Fig. 1(a)] we experimentally analyze the properties of OTO commutators [Figs. 1(b) and 1(c)], defined as $C_{AB}(t) \equiv \langle [A(t), B][A(t), B]^\dagger\rangle_\beta$, where

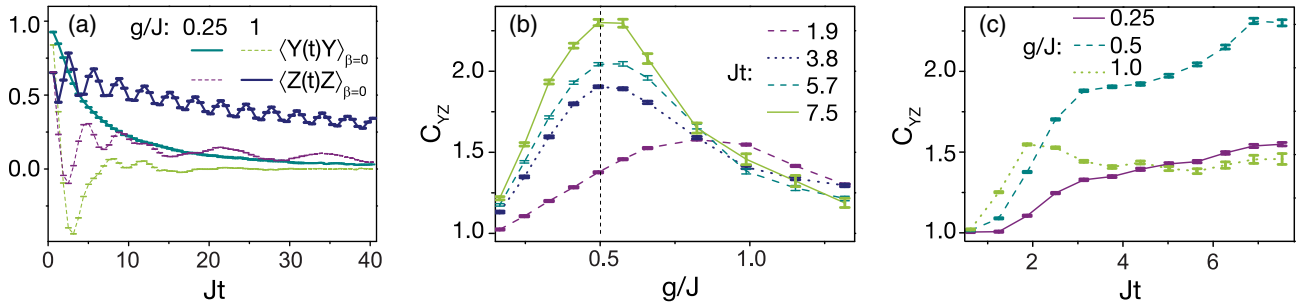

FIG. 1. (a) Distinct behavior for transverse (Y) and longitudinal (Z) magnetization: $\langle Y(t)Y\rangle_{\beta=0}$ at $g/J = 0.25$ shows a fast decay as a function of time, indicating erasure of initial memory. $\langle Z(t)Z\rangle_{\beta=0}$ at $g/J = 1$ shows instead slow nonergodic dynamics with periodic oscillations. In the opposite regimes (dashed lines) both correlations quickly decay to zero. Experimentally measured OTO commutator, C_{YZ}, as a function of transverse field strength (b) and normalized time (c). We observe the fastest growth around $g/J = 0.5$ [marked by a dashed line in (b)]. Here and in the rest of the Letter, error bars are determined from the noise in the free induction decay (see Supplemental Material [50] for details on the experimental scheme).

$A(t) = U(t)AU(t)^\dagger$, with $U(t) = e^{-i\hat{H}t}$ and $\hat{H}$ being the system Hamiltonian. Here $\langle\cdots\rangle_\beta = \mathrm{Tr}(e^{-\beta\hat{H}}\cdots)/\mathrm{Tr}(e^{-\beta\hat{H}})$ denotes the ensemble average at the inverse temperature β. The OTO commutator contains a term with an unconventional temporal order, the OTO correlator $F(t) \equiv \langle A^\dagger(t)B^\dagger A(t)B\rangle_\beta$, which can provide a more accurate description of operator scrambling than, e.g., Loschmidt echoes [67–74]. We exploit our ability to engineer a time reversal of the Hamiltonian in Eq. (1) to measure the OTO commutator of extensive observables [75], as we explain in the following.

In room temperature NMR experiments, the initial state for a chain of L spins is described by the density matrix $\rho(0) \approx (\mathbb{1} - \epsilon Z)/2^L$, with $\epsilon \sim 10^{-5}$. Since the identity operator does not contribute to any measurable signal, we only care about the deviation from it, $\delta\rho = 2Z/\sqrt{L}$, which has been normalized such that $\mathrm{Tr}(\delta\rho^2)/2^L = 1$. The mixed initial state enables the experimental study of two-point correlators and OTO commutators in a straightforward way. Since $\delta\rho(0)$ is usually the collective spin magnetization pointing in some direction, $\mathcal{O}_\mathbf{n} = \sum_j \mathbf{n}\cdot\mathbf{S}_j$ and we can measure the collective magnetization around any axis, the typical signal is the two-point correlation, $4\mathrm{Tr}[U(t)\delta\rho(0)U^\dagger(t)\mathcal{O}_\mathbf{n}]/(2^L L) \equiv \langle\mathcal{O}_\mathbf{n}(t)\mathcal{O}_\mathbf{n}\rangle_{\beta=0}$. That is, in our experiments, the (deviation of) the density matrix plays the role of an observable for an effective simulated system at infinite temperature. Crucially, however, the "simulated observable" $\delta\rho$ will thermalize at long times under the strong driving, $\langle\delta\rho(t)\rangle = 0$; this enables distinguishing the prethermal regimes from the expected (zero) signal at long times due to the eventual thermalization. MQC experiments [46,76,77] measure the overlap of the time-evolved density matrix, $\delta\rho(t) = U(t)\delta\rho(0)U^\dagger(t)$, with itself after a collective rotation. The overall measured signal can be expressed as

$$S_\phi = 2^{-L}\mathrm{Tr}[e^{-i\phi\mathcal{O}_\mathbf{n}}\delta\rho(t)e^{i\phi\mathcal{O}_\mathbf{n}}\delta\rho(t)]. \tag{2}$$

Taking a discrete Fourier transform of S_ϕ with respect to ϕ yields the MQC intensities: $S_\phi = \sum_q e^{-iq\phi}I_q$. Expanding S_ϕ in powers of ϕ, it can be shown that $\mathrm{Tr}([\delta\rho(t),\mathcal{O}_\mathbf{n}]^2)/2^L = -\sum_q q^2 I_q$. Setting $\delta\rho(0) = \mathcal{O}_{\mathbf{n}'}$, we can write

$$C_{\mathcal{O}_{\mathbf{n}'}\mathcal{O}_\mathbf{n}}(t) = \frac{4}{L}\langle|[\mathcal{O}_{\mathbf{n}'}(t),\mathcal{O}_\mathbf{n}]|^2\rangle_{\beta=0} = \sum_q q^2 I_q(t). \tag{3}$$

Equation (3) is the central idea of our experiments: by measuring the second moment of the MQC intensities encoded in $\delta\rho(t)$ along $\mathcal{O}_\mathbf{n}$ one can obtain the OTO commutator between $\mathcal{O}_{\mathbf{n}'}(t)$ and $\mathcal{O}_\mathbf{n}$ as if the system were at infinite temperature [78]. Equation (3) was first derived in a different context in Ref. [79] for NMR systems. When applied to pure states, it relates the second moment of the MQC distribution to the quantum Fisher information [47].

To study the system dynamics after a quench to Hamiltonian Eq. (1), we experimentally measure the OTO commutator $C_{YZ} \equiv 4L^{-1}\langle|[Y(t),Z]|^2\rangle_{\beta=0}$ for various transverse field strengths and times [see Figs. 1(b) and 1(c)]. First note that in the limit $g \to \infty$, Z is a conserved quantity thus making C_{YZ} constant. In Fig. 1(c) we observe that for a large but finite transverse field C_{YZ} stops growing at an early time, revealing that Z is approaching the emergent conserved quantity Z_{pre}—as also indicated by the slow decay and persistent oscillation of the two point correlator $\langle Z(t)Z\rangle_{\beta=0}$ [Fig. 1(a)]. For the small transverse field, instead, C_{YZ} keeps increasing, suggesting a faster heating rate [Fig. 1(c)]. We note that in the limit of exactly no transverse field, Y is a conserved quantity thus making C_{YZ} constant. However, as long as a small field is introduced the heating rate increases quadratically $\propto(J/g)^2$ [64] until the field strength induces a transition to the exponential prethermal regime; we thus observe a maximum of C_{YZ} at around $g/J \approx 0.5$ [Fig. 1(b)]. This maximum is due to a competition between the two terms in the Hamiltonian, similar to the competition between two phases at a quantum critical point. Indeed, the ground state shows a quantum phase transition, which is however at $g/J \approx 0.9$ [60]. Thus, although OTO commutators have been proposed to study quantum criticality at low enough temperature [80], here the link between information scrambling and the quantum critical point is unclear. The dynamics for an initial effective infinite temperature state is further indicated by the decay of $\langle Y(t)Y\rangle_{\beta=0}$ in Fig. 1(a) and additional OTO commutators presented below. Control imperfection (such as pulse errors and rf transients) and decoherence due to the open system dynamics preferentially affect the higher quantum coherences of large spin correlations. In addition, for longer time the interchain coupling becomes non-negligible so the system is no longer one dimensional [81].

To gain further insight into the differences between the quadratic and exponential heating regimes, we experimentally measure C_{ZZ} and C_{YY}, as shown in Fig. 2(a). Because these OTO commutators fluctuate significantly in time, we average them at six different times. As g increases, $Z(t)$ approaches the prethermal conserved quantity Z_{pre}, which itself gets close to Z, and C_{ZZ} gets smaller. This behavior is only observed for OTO commutators involving at least one operator that overlaps with the emergent conserved quantity, while other commutators, such as C_{YY}, keep growing as if the system were thermal, regardless of the transverse field strength (with the exception of exactly zero field, $g = 0$).

While we cannot directly measure Z_{pre}, the time-averaged operator $\bar{Z} = t_{\mathrm{pre}}^{-1}\int_0^{t_{\mathrm{pre}}} Z(t)dt$ (where t_{pre} is the

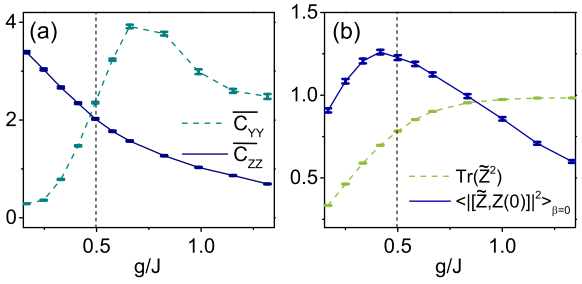

FIG. 2. (a) Experimentally averaged C_{YY} (dashed) and C_{ZZ} (solid) as a function of transverse field strength. (b) Experimentally measured $\mathrm{Tr}(\tilde{Z}^2)$ (dashed) and $\langle|[\tilde{Z},Z(0)]|^2\rangle_{\beta=0}$ (solid) versus transverse field strength. The time average is taken over the values $Jt = 3.77,\ 5.02,\ 6.28,\ 7.54,\ 8.80,\ 10.05$, with the longest time corresponding to 16 cycles (1.54 ms).

timescale over which the prethermal conserved quantity is present) captures its essential features [82]. Indeed, we can generally write $Z(t) = Z_{\mathrm{pre}} + U(t)(Z - Z_{\mathrm{pre}})U(t)^{\dagger}$: then, in the prethermal regime, the second term is small and fluctuates, yielding $\bar{Z} \approx Z_{\mathrm{pre}}$ after time average. We can approximate $\bar{Z}$ with a discrete time average, $\tilde{Z} = \sum_{n=1}^{N} Z(t_n)/N$, by independently varying the forward and backward evolution times in the MQC protocol (see in the Supplemental Material [50] for details on the experiments and for a comparison between $\bar{Z}$ and $\tilde{Z}$). Figure 2(b) shows that $\mathrm{Tr}(\tilde{Z}^2)/\mathrm{Tr}(Z(0)^2) \to 1$ as g increases, because the time-varying part of $Z(t)$ is very small for large g. Furthermore, $4/L\langle|[\tilde{Z},Z(0)]|^2\rangle_{\beta=0}$ approaches zero at large g, suggesting that $\lim_{g\to\infty}\tilde{Z} = Z$.

To support our interpretation of the experimental results, we numerically construct the prethermal Hamiltonian in the large field limit, showing that indeed $Z_{\mathrm{pre}} \approx Z$ is an emergent constant of motion. The prethermal Hamiltonian can be expanded in powers of $\epsilon = J/g$

$$H_{\mathrm{pre}} = Z' + \sum_{n=1}^{n_M} \epsilon^n h^{(n)}, \tag{4}$$

and numerically evaluated up to order n_M (see Section IV in the Supplemental Material [50]). It has been shown [34] that for generic many-body systems the series in Eq. (4) might not converge as $n_M \to \infty$, but there exists an optimal order n when truncating the series, so that H_{pre} is most similar to H. If the system Hamiltonian does indeed support prethermalization, we expect its eigenvalues E_m to be close to the prethermal Hamiltonian ones, E_m^{pre}. We thus calculate the eigenvalue difference $r \equiv \mathrm{mean}_m(E_m - E_m^{\mathrm{pre}})/L$ (where m labels the eigenvalues in ascending order), expecting r to converge to zero only in the prethermal regime. Figure 3(a) shows r as a function of maximum truncation order n_M for different values of ϵ. For large g, $r \approx 0$ appears to converge up to the largest numerically accessible order, suggesting that H_{pre} is similar to H and there exists an approximately conserved quantity Z_{pre}. For small g however, r diverges, indicating that a prethermal Hamiltonian that conserves Z' cannot be found. The transition happens at around $g/J = 0.5$.

To further demonstrate that a conserved quantity emerges for large g, we simulate Z at large times $(Jt = 10^3)$ and decompose it according to the Hamming weight [9]

$$Z(Jt = 10^3) = \sqrt{2^{L-2}L}\sum_{k=1}^{L}\sum_{s=1}^{\zeta_k} b_k^s(Jt)\mathcal{B}_k^s, x \tag{5}$$

where $\mathcal{B}_k^s$ are operators composed of tensor products of k Pauli matrices and $L-k$ identity operators, and $\zeta_k \propto 3^k \times \binom{L}{k}$ labels the number of configurations with k non-identity Pauli operators. We define the Hamming weight of k-spin correlations as $f_k = \sum_{s=1}^{\zeta_k}[b_k^s]^2$, satisfying $\sum_{k=1}^{L} f_k = 1$. Figure 3(b) shows that for the small transverse

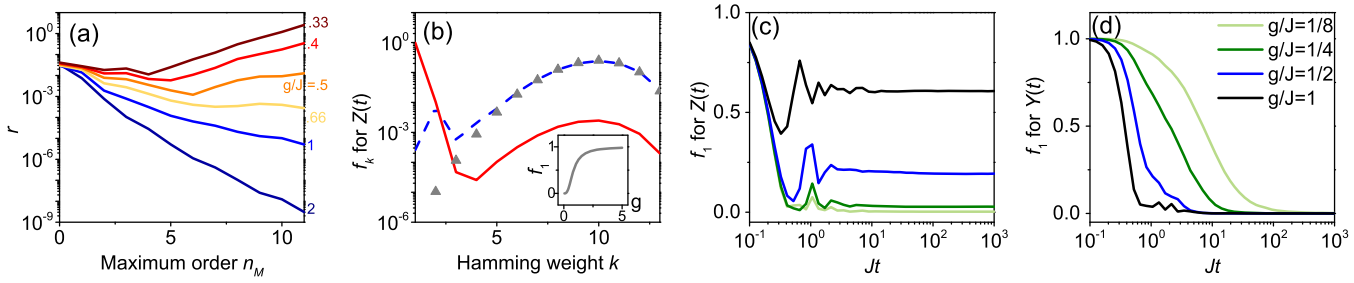

FIG. 3. Numerical characterization of the prethermal Hamiltonian. (a) Eigenvalue difference r with respect to maximum order n_M for different values of g/J. r shows a divergence, up to a maximum field value $g/J = 0.5$. (b) Decomposition of $Z(t)$ (obtained by exact diagonalization) at $Jt = 10^3$ according to the operator Hamming weight: f_k is the contribution of all possible spin correlations with Hamming weight k. For small fields, $g/J = 0.05$ (dashed line), the result follows closely the distribution (triangles) obtained randomly sampling all possible operators. For large fields, $g/J = 5$ (solid line) there is a significant contribution of single-body terms, related to the quasiconserved quantity Z_{pre}. In the inset: f_1 as a function of g. f_1 for $Z(t)$ (c) and $Y(t)$ (d) as a function of normalized time, showing the nonthermal behavior of Z at large g/J, while Y is always thermal even for small g/J. The system size is $L = 12$ for (a) and 13 for (b)–(d).

field f_k is approximately proportional to ζ_k, suggesting that all possible operators $\mathcal{B}_k^s$ have the same weight at very late time $Jt = 10^3$, in agreement with the eigenvalue thermalization hypothesis [84–87]. The result is qualitatively different for $g \gg 1$, where a significant one-body term, f_1, exists even at $Jt = 10^3$, signifying the failure of thermalization and the emergence of the conserved quantity Z_{pre}. We thus study f_1 as a function of time. For small fields, $g/J \leq 0.5$, the contribution of f_1 in $Z(t)$ relaxes from one to zero, as shown in Fig. 3(c). For large g/J, instead, f_1 reaches a nonzero, quasiequilibrium value, signaling the prethermal regime. We do not see the final thermalizing stage in the numerics, possibly because small systems, $L = 13$, do not fully thermalize [88]. On the other hand, while Y is conserved at exactly zero field ($g = 0$), as soon as a small transverse field is introduced the contribution of f_1 to $Y(t)$ decays to zero [Fig. 3(d)]. This indicates that the slow dynamics observed for $Y(t)$ at small g is not protected by the prethermal conserved quantity in the same way as $Z(t)$ at large g, and will thus thermalize on timescales much shorter than the exponentially long t_{pre}. The quantitative difference between f_1 for $Y(t)$ and $Z(t)$ can be approximately observed by measuring the two-point correlations $\langle Z(t)Z\rangle_{\beta=0}$ and $\langle Y(t)Y\rangle_{\beta=0}$. As shown in Fig. 1(a), in the small field regime $\langle Y(t)Y\rangle$ decreases rapidly as a function of time, suggesting that $f_1(t)$ of $Y(t)$ is not a (prethermal) conserved quantity that persists to exponentially long time [89]. In stark contrast, $\langle Z(t)Z\rangle$ shows a slow decay with periodic oscillations, suggesting that $f_1(t)$ of $Z(t)$ is mostly conserved, consistent with prethermalization at large g/J [90].

In conclusion, we studied the out-of-equilibrium dynamics of the transverse field dipolar interaction in a solid-state NMR quantum simulator. Using MQC techniques, we measured OTO commutators to reveal a distinct dynamics in the high and low field regimes, and identified the former as prethermal regimes which does not thermalize on practically accessible timescales. In the prethermal regime, when one of the OTO operators is close to the emergent quasiconserved quantity, the OTO commutator saturates at an early time, while it keeps increasing in the opposite regime, with a transition at about $g/J = 0.5$. We further validate our experimental results numerically, by constructing the prethermal Hamiltonian and verifying the emergence of a conserved quantity at high field. We demonstrate the value of OTO commutators in investigating nonequilibrium quantum thermodynamics, while also providing a method to experimentally measure OTO commutators that could be extended to other experimental platforms. Similar techniques could be used for example to explore other many-body phenomena, such as localization, dynamics phase transition, and information scrambling, paving the way to a more comprehensive understanding of out-of-equilibrium quantum many-body systems.

We thank N. Halpern, D. Huse, and I. Cirac for insightful discussions. This work was supported in part by the National Science Foundation PHY1734011 and PHY1915218.

K. X. W. and P. P. contributed equally to this work.

*pcappell@mit.edu

[1] A. M. Kaufman, M. E. Tai, A. Lukin, M. Rispoli, R. Schittko, P. M. Preiss, and M. Greiner, Science **353**, 794 (2016).
[2] G. Kucsko, S. Choi, J. Choi, P. C. Maurer, H. Zhou, R. Landig, H. Sumiya, S. Onoda, J. Isoya, F. Jelezko, E. Demler, N. Y. Yao, and M. D. Lukin, Phys. Rev. Lett. **121**, 023601 (2018).
[3] D. Basko, I. Aleiner, and B. Altshuler, Ann. Phys. (Amsterdam) **321**, 1126 (2006).
[4] D. M. Basko, I. L. Aleiner, and B. L. Altshuler, Phys. Rev. B **76**, 052203 (2007).
[5] R. Nandkishore and D. A. Huse, Annu. Rev. Condens. Matter Phys. **6**, 15 (2015).
[6] M. Schreiber, S. S. Hodgman, P. Bordia, H. P. Lüschen, M. H. Fischer, R. Vosk, E. Altman, U. Schneider, and I. Bloch, Science **349**, 842 (2015).
[7] J. Smith, A. Lee, P. Richerme, B. Neyenhuis, P. W. Hess, P. Hauke, M. Heyl, D. A. Huse, and C. Monroe, Nat. Phys. **12**, 907 (2016).
[8] J.-Y. Choi, S. Hild, J. Zeiher, P. Schauß, A. Rubio-Abadal, T. Yefsah, V. Khemani, D. A. Huse, I. Bloch, and C. Gross, Science **352**, 1547 (2016).
[9] K. X. Wei, C. Ramanathan, and P. Cappellaro, Phys. Rev. Lett. **120**, 070501 (2018).
[10] A. Lukin, M. Rispoli, R. Schittko, M. E. Tai, A. M. Kaufman, S. Choi, V. Khemani, J. Léonard, and M. Greiner, Science **364**, 256 (2019).
[11] V. Khemani, A. Lazarides, R. Moessner, and S. L. Sondhi, Phys. Rev. Lett. **116**, 250401 (2016).
[12] C. W. vonKeyserlingk, V. Khemani, and S. L. Sondhi, Phys. Rev. B **94**, 085112 (2016).
[13] D. V. Else, B. Bauer, and C. Nayak, Phys. Rev. Lett. **117**, 090402 (2016).
[14] R. Moessner and S. L. Sondhi, Nat. Phys. **13**, 424 (2017).
[15] K. Sacha and J. Zakrzewski, Rep. Prog. Phys. **81**, 016401 (2018).
[16] N. Y. Yao, A. C. Potter, I. D. Potirniche, and A. Vishwanath, Phys. Rev. Lett. **118**, 030401 (2017).
[17] J. Zhang, P. W. Hess, A. Kyprianidis, P. Becker, A. Lee, J. Smith, G. Pagano, I. D. Potirniche, A. C. Potter, A. Vishwanath, N. Y. Yao, and C. Monroe, Nature (London) **543**, 217 (2017).
[18] S. Choi, J. Choi, R. Landig, G. Kucsko, H. Zhou, J. Isoya, F. Jelezko, S. Onoda, H. Sumiya, V. Khemani, C. von Keyserlingk, N. Y. Yao, E. Demler, and M. D. Lukin, Nature (London) **543**, 221 (2017).
[19] W. W. Ho, S. Choi, M. D. Lukin, and D. A. Abanin, Phys. Rev. Lett. **119**, 010602 (2017).
[20] J. Zhang, G. Pagano, P. W. Hess, A. Kyprianidis, P. Becker, H. Kaplan, A. V. Gorshkov, Z.-X. Gong, and C. Monroe, Nature (London) **551**, 601 (2017).

[21] E. A. Yuzbashyan, O. Tsyplyatyev, and B. L. Altshuler, Phys. Rev. Lett. **96**, 097005 (2006).

[22] M. Heyl, A. Polkovnikov, and S. Kehrein, Phys. Rev. Lett. **110**, 135704 (2013).

[23] B. Žunković, M. Heyl, M. Knap, and A. Silva, Phys. Rev. Lett. **120**, 130601 (2018).

[24] N. Fläschner, D. Vogel, M. Tarnowski, B. S. Rem, D.-S. Lühmann, M. Heyl, J. C. Budich, L. Mathey, K. Sengstock, and C. Weitenberg, Nat. Phys. **14**, 265 (2018).

[25] P. Jurcevic, H. Shen, P. Hauke, C. Maier, T. Brydges, C. Hempel, B. P. Lanyon, M. Heyl, R. Blatt, and C. F. Roos, Phys. Rev. Lett. **119**, 080501 (2017).

[26] N. Y. Yao, C. R. Laumann, J. I. Cirac, M. D. Lukin, and J. E. Moore, Phys. Rev. Lett. **117**, 240601 (2016).

[27] Z. Papić, E. M. Stoudenmire, and D. A. Abanin, Ann. Phys. (Amsterdam) **362**, 714 (2015).

[28] A. Smith, J. Knolle, D. L. Kovrizhin, and R. Moessner, Phys. Rev. Lett. **118**, 266601 (2017).

[29] A. A. Michailidis, M. Žnidarič, M. Medvedyeva, D. A. Abanin, T. Prosen, and Z. Papić, Phys. Rev. B **97**, 104307 (2018).

[30] J. Berges, S. Borsányi, and C. Wetterich, Phys. Rev. Lett. **93**, 142002 (2004).

[31] M. Gring, M. Kuhnert, T. Langen, T. Kitagawa, B. Rauer, M. Schreitl, I. Mazets, D. Adu Smith, E. Demler, and J. Schmiedmayer, Science **337**, 1318 (2012).

[32] D. V. Else, P. Fendley, J. Kemp, and C. Nayak, Phys. Rev. X **7**, 041062 (2017).

[33] D. V. Else, B. Bauer, and C. Nayak, Phys. Rev. X **7**, 011026 (2017).

[34] D. A. Abanin, W. De Roeck, W. W. Ho, and F. Huveneers, Phys. Rev. B **95**, 014112 (2017).

[35] B. Neyenhuis, J. Smith, A. C. Lee, J. Zhang, P. Richerme, P. W. Hess, Z. X. Gong, A. V. Gorshkov, and C. Monroe, Sci. Adv. **3**, e1700672 (2017).

[36] A. I. Larkin and Y. N. Ovchinnikov, Sov. Phys. JETP **28**, 1200 (1969).

[37] A. Kitaev, in *A simple model of quantum holography, The Kavli Institute for Theoretical Physics KITP, University of California, 2015*, http://online.kitp.ucsb.edu/online/entangled15/kitaev/.

[38] A. Kitaev and S. J J. Suh, J. High Energy Phys. 18 (2018) 183.

[39] M. Garttner, J. G. Bohnet, A. Safavi-Naini, M. L. Wall, J. J. Bollinger, and A. M. Rey, Nat. Phys. **13**, 781 (2017).

[40] J. Li, R. Fan, H. Wang, B. Ye, B. Zeng, H. Zhai, X. Peng, and J. Du, Phys. Rev. X **7**, 031011 (2017).

[41] K. A. Landsman, C. Figgatt, T. Schuster, N. M. Linke, B. Yoshida, N. Y. Yao, and C. Monroe, Nature (London) **567**, 61 (2019).

[42] R. Fan, P. Zhang, H. Shen, and H. Zhai, Sci. Bull. **62**, 707 (2017).

[43] Y. Chen, arXiv:1608.02765.

[44] Y. Huang, Y. L. Zhang, and X. Chen, Ann. Phys. (Amsterdam) **529**, 1600318 (2017).

[45] K. Slagle, Z. Bi, Y.-Z. You, and C. Xu, Phys. Rev. B **95**, 165136 (2017).

[46] M. Munowitz and A. Pines, *Principle and Applications of Multiple-Quantum NMR*, edited by I. Prigogine and S. Rice, Advances in Chemical Physics Vol. 66 (Wiley, New York, 1975).

[47] M. Gärttner, P. Hauke, and A. M. Rey, Phys. Rev. Lett. **120**, 040402 (2018).

[48] D. V. Else, B. Bauer, and C. Nayak, Phys. Rev. X **7**, 011026 (2017).

[49] W. V. der Lugt and W. Caspers, Physica (Utrecht) **30**, 1658 (1964).

[50] See Supplemental Material at http://link.aps.org/supplemental/10.1103/PhysRevLett.123.090605 additional details on the theoretical model, simulations and experiments.

[51] P. Cappellaro, C. Ramanathan, and D. G. Cory, Phys. Rev. Lett. **99**, 250506 (2007).

[52] W. Zhang, P. Cappellaro, N. Antler, B. Pepper, D. G. Cory, V. V. Dobrovitski, C. Ramanathan, and L. Viola, Phys. Rev. A **80**, 052323 (2009).

[53] C. Ramanathan, P. Cappellaro, L. Viola, and D. G. Cory, New J. Phys. **13**, 103015 (2011).

[54] F. C. Alcaraz, M. N. Barber, M. T. Batchelor, R. J. Baxter, and G. R. W. Quispel, J. Phys. A **20**, 6397 (1987).

[55] E. K. Sklyanin, J. Phys. A **21**, 2375 (1988).

[56] Y. Wang, W.-L. Yang, J. Cao, and K. Shi, *Off-Diagonal Bethe Ansatz for Exactly Solvable Models* (Springer, New York, 2016).

[57] D. K. Sodickson and J. S. Waugh, Phys. Rev. B **52**, 6467 (1995).

[58] W. Zhang and D. G. Cory, Phys. Rev. Lett. **80**, 1324 (1998).

[59] D. Jyoti, arXiv:1711.01948.

[60] A. Isidori, A. Ruppel, A. Kreisel, P. Kopietz, A. Mai, and R. M. Noack, Phys. Rev. B **84**, 184417 (2011).

[61] U. Haeberlen and J. Waugh, Phys. Rev. **175**, 453 (1968).

[62] Note that the form of this Hamiltonian is reminiscent of a spin-locking dipolar interaction in NMR [63].

[63] C. P. Slichter, *Principles of Magnetic Resonance*, 3rd ed. (Springer-Verlag, 1996).

[64] K. Mallayya, M. Rigol, and W. De Roeck, Phys. Rev. X **9**, 021027 (2019).

[65] D. V. Else, P. Fendley, J. Kemp, and C. Nayak, Phys. Rev. X **7**, 041062 (2017).

[66] D. Abanin, W. De Roeck, W. W. Ho, and F. Huveneers, Commun Math. Phys. **354**, 809 (2017).

[67] H. T. Quan, Z. Song, X. F. Liu, P. Zanardi, and C. P. Sun, Phys. Rev. Lett. **96**, 140604 (2006).

[68] B. Swingle, G. Bentsen, M. Schleier-Smith, and P. Hayden, Phys. Rev. A **94**, 040302(R) (2016).

[69] E. Hahn, Phys. Rev. **80**, 580 (1950).

[70] W.-K. Rhim, A. Pines, and J. S. Waugh, Phys. Rev. B **3**, 684 (1971).

[71] S. Zhang, B. H. Meier, and R. R. Ernst, Phys. Rev. Lett. **69**, 2149 (1992).

[72] M. F. Andersen, A. Kaplan, and N. Davidson, Phys. Rev. Lett. **90**, 023001 (2003).

[73] T. Gorin, T. Prosen, T. H. Seligman, and M. Žnidarič, Phys. Rep. **435**, 33 (2006).

[74] T. Prosen, T. H. Seligman, and M. Žnidarič, Prog. Theor. Phys. Suppl. **150**, 200 (2003).

[75] I. Kukuljan, S. Grozdanov, and T. Prosen, Phys. Rev. B **96**, 060301(R) (2017).

[76] J. Baum, M. Munowitz, A. N. Garroway, and A. Pines, J. Chem. Phys. **83**, 2015 (1985).

[77] C. Ramanathan, H. Cho, P. Cappellaro, G. S. Boutis, and D. G. Cory, Chem. Phys. Lett. **369**, 311 (2003).
[78] Notice that exchanging $\mathcal{O}_{\mathbf{n}'}$ and $\mathcal{O}_{\mathbf{n}}$ will result in a different MQC distribution I_q, however its second moment remains the same.
[79] A. Khitrin,, Chem. Phys. Lett. **274**, 217 (1997).
[80] H. Shen, P. Zhang, R. Fan, and H. Zhai, Phys. Rev. B **96**, 054503 (2017).
[81] W. Zhang, P. Cappellaro, N. Antler, B. Pepper, D. G. Cory, V. V. Dobrovitski, C. Ramanathan, and L. Viola, Phys. Rev. A **80**, 052323 (2009).
[82] In the limit $t_{\mathrm{pre}} \to \infty$, $\bar{Z}$ becomes an exact integral of motion and it has also recently been proposed as an experimentally accessible observable for detecting MBL to ergodic phase transition [83].
[83] A. Chandran, I. H. Kim, G. Vidal, and D. A. Abanin, Phys. Rev. B **91**, 085425 (2015).
[84] P. Hosur and X.-L. Qi, Phys. Rev. E **93**, 042138 (2016).
[85] M. Rigol, V. Dunjko, and M. Olshanii, Nature (London) **452**, 854 (2008).
[86] J. M. Deutsch, Phys. Rev. A **43**, 2046 (1991).
[87] M. Srednicki, Phys. Rev. E **50**, 888 (1994).
[88] F. Machado, G. D. Meyer, D. V. Else, C. Nayak, and N. Y. Yao, arXiv:1708.01620.
[89] We further numerically demonstrate in the Supplemental Material that H is unlikely to be in a prethermal regime with respect to NN Ising interactions $\sum_j S_y^j S_y^{j+1}$, the dominant term in H_{tdip} for small values of g.
[90] Taking the average over time, also shows that $\bar{Z} \approx Z$ in the prethermal regime.